Mechanics of Thin, Flexible, Translating Media and Their Interactions with Surrounding Air

Sinan Müftü
Associate Professor
Northeastern University, Department of Mechanical and Industrial Engineering, Boston, MA 02115, USA

Thin, flexible, continuous structures known as webs are used in a wide range of industrial applications. These structures interact with the surrounding air in beneficial or detrimental ways, depending on the application and the process parameters. A review of the literature related to modeling and experimental work on (mostly) the steady state fluid-structure interactions is given. Equilibrium equations of web mechanics, and the inertia dominated and viscosity dominated air flows are presented. Simulation examples from four different industrial applications; web/air-bar interactions; roller/web interactions for permeable and impermeable webs; and the flat-top recording-head/magnetic-tape interactions, are presented.

Key Words: Web mechanics, Turn bar, Air reverser, Air bar, Roll-to-roll manufacturing, Air lubrication, Fluid-structure interaction

1. Introduction

Thin, flexible, continuous materials known as webs are encountered in a wide range of industrial settings. Roll-to-roll (RR) manufacturing provides a cost effective method to produce large quantities of a product. Classically, making of paper and photographic film, linear and helical magnetic tape recording, processing of aluminum foils and packaging products all require handling of these thin materials. Recently, RR methods were introduced to manufacturing of polymer light emitting diodes (PLEDs) and/or thin film transistors (TFTs) on thin plastic substrates. Among the potential applications of these new technologies are flexible computer displays, light sources, television sets, and wearable computers with diverse civilian and military uses. Depending on the application, webs can encounter one or many rollers, fixed guides, coaters, driers during manufacturing or operational handling. In this paper a literature review of the papers related to the mechanics of some of the challenges caused by these interactions, is presented.

Mechanics of flexible webs has received considerable attention in the last half-century. Wickert and Mote[53] review the literature of *stability* of the out-of-plane vibrations of translating continuous media. Dynamics of *lateral web motion* has been analyzed by Shelton[48] and Benson,[2] among many others. More recently, Taylor et al.[21,51] and Machida and Wickert.[27] investigated the lateral tape motion for linear tape drives. Models for the mechanics of *wound rolls* have been developed by Altman,[1] Hakiel,[17] Benson[3] and more recently by Wickert et al. [22,54]

The fluid structure interaction between the flexible webs and surrounding air is typically unavoidable and gives rise to interesting problems. A flexible web drags the surrounding air into the guide-web interface while it travels over rollers or stationary guides. The resulting phenomenon is known as the *foil bearing* problem and has been extensively studied.[8,37,17] The foil bearing problem stems from low Reynolds number effects hence the fluid mechanics is governed by the Reynolds lubrication equation.[8]

Dynamic stability of a thin web traveling between rollers can be significantly affected by the surrounding air, as the mass of air is comparable to mass of the web.[23,41,42,43,44] The fundamental vibration frequencies of a traveling web attain lower values, when the surrounding air mass is coupled to the out-of-plane vibrations of the web.

An *air-bar* (Fig 1) is used in a web handling application where the transport direction of the web needs to be reversed without making contact with a rigid surface. In order to achieve this goal, the web is wrapped around a cylindrical drum with holes on its surface to provide a pressurized air layer under the web. In general the web is wrapped around the cylinder in a helical fashion with a helix angle β. This device allows the web transport direction to be changed by an angle 2β, and thus enables more flexibility on manufacturing floor layout.

A web guided by an ideal roller (Fig. 2), with a frictionless bearing, operating in vacuum should not experience any slip over the roller, if the friction coefficient between the web and the roller is greater than zero.[20] However, in practice, the air entrained in the web/roller interface causes *mixed lubrication* condition to develop. In this case, the web is supported partially by the rigid body contact of the asperities, and partially by the air layer; and, consequently the effective friction coefficient is reduced.[8,9,14,15,16,40,37,45,46] At sufficiently high web transport speed the effective friction coefficient can become zero.

The mixed lubrication is also encountered in the head-tape interface[25,29,50,55,56] In order to minimize the signal loss, modern tape recording applications require the tape to be in contact with the recording head, during the read/write operations. However, keeping the tape in contact with the head is a challenging task with cylindrically contoured heads, in which the mostly superambient air pressure in the head-tape interface, caused by the self-acting air bearing, tends to separate the tape from the head. It has been shown that when a *flat* recording head (Fig. 3) is used instead of a cylindrical one, reliable contact is obtained over the central region of the flat-head. [4,5 ,18,19,29,30,33,36]

In the rest of this paper the equations of static equilibrium for web deflections, as well as the fluid mechanics equations representing the air flow under the web, for different types of fluid-structure interactions will be introduced. Equations that represent the contact between a web and rigid surface, such as a roller, will not be reviewed here due to space limitations, but can be found in many references cited here.[18,20,24,25,45,55,56,57] Simulation examples from four different industrial applications; web/air-bar interactions; roller/web interactions for permeable and impermeable webs; and the flat-top recording-head/magnetic-tape interactions, will be presented.

2. Governing Equations of a Flexible Web

The govering equation for a thin flexible web wrapped around a surface, such as a turn bar, roller or tape recording head is presented. First, the general equation of static equilibrium in the out-of-plane direction is presented for a web wrapped around a cylinder in a helical fashion. This equation is then reduced for non-helical wrap and small deformations.

2.1 Helically Wrapped Web

In order to derive the equilibrium equations for a web in an air-bar application, the web deflections are measured with respect to the self-adjusting reference state, which is initially unknown[35]. Thus the web deflection equations become non-linear. The self-adjusting reference state is a cylindrical surface extending from the mid-line of the deflected web defined as $w_r(x) = w(x,L_x/2)$. The normal component of the web deflection is measured with respect to w_r and is indicated by, $\bar{w} = w - w_r$.

The geometry of a web wrapped at an oblique (helix) angle β around a cylinder of radius R_c is depicted in Figure 1a. The governing equations for the web displacements are expressed on the (x,y) coordinate system shown in Figure 1b.

A web wrapped around a cylindrical surface with a helix angle β represents a developable surface.[38,47] Web equilibrium equations are derived in curvilinear coordinates. The equations are written with respect to the initial reference configuration w_0, for an infinitely thin web. The curvilinear coordinates and the equilibrium equations with respect to this system are described by Rongen[47]. The equations of equilibrium are derived using the Kirchhoff-Love assumptions, which state that: a) The shell is in a state of plane stress, where the normal stress in the thickness direction of the shell is neglected; and, b) A fiber of the shell which is initially straight and normal to the middle surface, remains straight and normal to the middle surface after deformation.[52]

The mechanics of the web is described with respect to a set of curvilinear coordinates located on the web (x, y, n). By using moment curvature relations, the curvature tensor and the equations of equilibrium in curvilinear-coordinates, the governing equations are found as[38]:

$$N_{xx,x} + N_{xy,y} + F_x = 0,$$

$$N_{yx,x} + N_{yy,y} + F_y = 0,$$

$$D_b \nabla^4 \bar{w} - \left(w_{,xx} - \frac{\cos^2 \beta}{R_w} \right) N_{xx} - 2\left(w_{,xy} - \frac{\sin\beta\cos\beta}{R_w} \right) N_{xy} - \left(w_{,yy} - \frac{\sin^2 \beta}{R_w} \right) N_{yy} = p. \tag{1}$$

where β is the helix-angle, N_{ij} $(i, j = x, y)$ are the in-plane stress resultants, w is the out-of-plane web deflection, F_x and F_y are external forces acting in-plane directions, p is the external pressure, $\nabla^4 = (\nabla^2)^2$ is the biharmonic differential operator, subscripted commas represent partial derivation, $D_b = (Ec^3/12(1-\nu^2))$ is the bending rigidity of the web with elastic modulus E, Poisson's ratio ν, and thickness c, and $R_w = R_w(x,y)$ is the radius of curvature of the shell defined as,

$$R_w^{-1}(x,y) = \begin{cases} 0, & \text{for } x + y\tan\beta - L_1 < 0 \\ R^{-1}, & \text{for } x + y\tan\beta - L_1 \geq 0 \text{ and } x+y\tan\beta - L_2 \leq 0 \\ 0, & \text{for } x + y\tan\beta - L_2 > 0 \end{cases} \tag{2}$$

where L_1 and L_2 are the tangency points at $y = 0$.

In a typical web handling application, the web is pre-tensioned to a value T in the longitudinal direction. It is assumed that, in the undeformed state, only T exists as in-plane stress, when the web is wrapped around the cylinder. The in-plane stress resultants after deformation are indicated as follows,

$$N_{xx} = T + N'_{xx}, \quad N_{yy} = N'_{yy}, \quad N_{xy} = N'_{xy}, \tag{3}$$

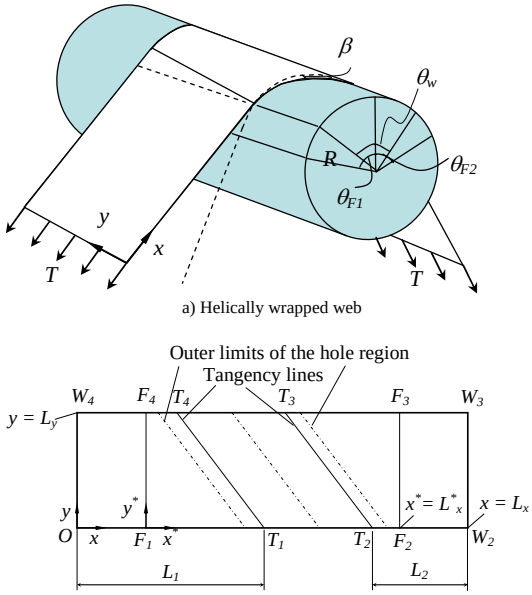

Figure 1. The helically wrapped air-bar model

A simplified equation which represents the equilibrium of out-of-plane force resultants and bending moments can be obtained by considering that N'_{xx} can be evaluated in terms of deformations by using the strain-displacement relations, and the constitutive relation. This gives the in-plane stress resultant in the longitudinal direction as:[38]

$$N_{xx} = T + D_t \left[\frac{\bar{w}}{R_w}\cos^2\beta + \frac{1}{2}\bar{w}_{,x}^2 + \nu\left(\frac{\bar{w}}{R_w}\sin^2\beta + \frac{1}{2}\bar{w}_{,y}^2 \right) \right] \tag{4}$$

where D_t $(= Ec/(1-\nu^2))$ is the in-plane stiffness of the web. Then the equation of equilibrium for a flexible web wrapped around a cylindrical drum with a helix angle β becomes:

$$D_b \nabla^4 \bar{w} + D_t \frac{\left(\cos^4\beta + \nu\cos^2\beta\sin^2\beta\right)\bar{w}}{R_w^2(x,y)} - T w_{,xx} = p - \frac{T\cos^2\beta}{R_w} \tag{5}$$

Note that for $\beta = 0$ this equation reduces to the same web equilibrium equation derived for the case of no helix angle.[35]

The web is supported by a roller on each of its two longitudinal ends, where the boundary conditions are typically assumed to be simple-support conditions; and, the web is free on its lateral edges where free boundary conditions are applied. [35]

2.2 Cylindrically Wrapped Web

In general, a web interacting with a roller is typically wrapped with zero helix angle. The web equilibrium equations are, then obtained by setting $\beta = 0$. For modeling the foil bearing problem, the reference state adjustment as described in Eqn (1) was used by Ducotey and Good.[9] A fixed reference state adjustment to account for initial straining due to contact with tall asperities has also been utilized.[37,46] In case rigid body contact exists between the web and the underlying structure contact pressure is added to the right hand side of Eqn (1), and calculated as demonstrated in.[18,20,24,25,45,55,57] In case the variation of web deflection and/or air flow in the lateral direction is negligable, then the y-coordinate dependence of Eqn (1) can be omitted.

3. Equations of Fluid Mechanics

The fluid mechanics in the web/air-bar interface is dominated by inertial effects[31,32]. In contrast, the fluid mechanics in the web/roller or head/tape interface is dominated by viscous effects. Depending on the problem considered, both of these equations can be considered 2D in the plane of the web, or the side flow can be be neglected by assuming that the fluid domain is infinitely wide.

In both situations the fluid and the structure domains are coupled through the clearance $h(x,y)$ between the web and the air-bar. This variable depends on the initial clearance $\delta(x,y)$ and the web displacement $w(x,y)$ as follows:

$$h(x, y) = w(x, y) + \delta(x, y) \tag{6}$$

The initial clearance in the downstream and upstream sides of the web is obtained by calculating the web-to-cylinder distance. In the wrap region, the initial clearance is zero (Fig. 2).

3.1 Fluid Mechanics of the Air Reverser

The steady state form of the equations governing the fluid mechanics of air, in the clearance between the web and the turn are modeled as 2D, in the plane of the web.[31,32] The flow is turbulent in the web-reverser clearance, as indicated by the Reynolds number, $\mathrm{Re} = \rho V h/\mu \approx 5200$[32]. The flow velocities u^* and v^* in the x^* and y^* directions, respectively, are averaged in the direction of the clearance height, and the flow component in the z^* direction is neglected. The effect of the air coming into the interface through the holes is modeled as a distributed source, indicated by $\alpha(x^*,y^*)$. Velocity of air U coming through each hole is a function of the supply pressure inside the reverser p_0 and the local pressure of air p:

$$U = \kappa U_0 (1 - p / p_0)^{1/2} \tag{7}$$

where the reference discharge velocity is $U_0 = (p_0/2\rho)^{1/2}$. 2D flow assumption is invalid near each hole, and losses due to discharge are represented with the discharge coefficient κ, whose value lies in the range (0,1]. The conservation of mass is given by,

$$\frac{\partial h u^*}{\partial x^*} + \frac{\partial h v^*}{\partial y^*} = \alpha U , \tag{8}$$

where the term on the right hand side represents the mass of air coming into the interface through the air holes. The conservation of momentum in the x^* and y^* directions is represented by the following two equations,

$$\rho\left(u^* \frac{\partial u^*}{\partial x^*} + v^* \frac{\partial u^*}{\partial y^*}\right) + \frac{\partial p}{\partial x^*} - \mu\left(\frac{4}{3}\frac{\partial^2 u^*}{\partial x^{*2}} + \frac{\partial^2 u^*}{\partial y^{*2}} + \frac{1}{3}\frac{\partial^2 v^*}{\partial x^* \partial y^*}\right) + 2\frac{\tau_{zx}}{h} + \alpha\rho U \frac{u^*}{h} = 0$$

$$\rho\left(u^* \frac{\partial v^*}{\partial x^*} + v^* \frac{\partial v^*}{\partial y^*}\right) + \frac{\partial p}{\partial y^*} - \mu\left(\frac{\partial^2 v^*}{\partial x^{*2}} + \frac{4}{3}\frac{\partial^2 v^*}{\partial y^{*2}} + \frac{1}{3}\frac{\partial^2 u^*}{\partial x^* \partial y^*}\right) + 2\frac{\tau_{z^* y^*}}{h} + \alpha\rho U \frac{v^*}{h} = 0 \tag{9}$$

where, ρ is the mass density, μ is the viscosity of air, and p is the air pressure averaged in the normal direction. The shear stresses $\tau_{z^* x^*}$ and $\tau_{z^* y^*}$ are found from the 1/7th-power-velocity distribution law for turbulent flow in a 2D-channel.[35, 49] The boundary condition for fluid is:

$$p + \frac{1}{2}\kappa_B (u^{*2} + v^{*2}) = 0 \quad \text{on } \Gamma_f \tag{10}$$

where κ_B is the boundary discharge coefficient, and Γ_f is the boundary of the fluid solution domain. The solution of this equation is obtained numerically.[31]

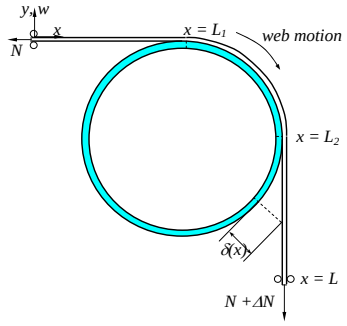

Figure 2. Geometric depiction of a web moving over a roller

3. 2 Reynolds Lubrication Equation

Typical value of the modified Reynolds number, Re* (= $\rho V h^2/L\mu$) in the interface of a roller and the web is on the order of 10^{-3}. Hence the fluid mechanics of the air flow is dominated by viscous effects. Therefore, the air flow is modeled by the Reynolds lubrication equation.

For tape handling applications, where the tape and head surfaces are very smooth, the effective clearance in the interface is on the order of the molecular mean free path (λ) of air. Then, the compressible Reynolds equation with slip flow corrections is used to model the air flow:

$$\nabla.\left\{ph^3 Q_r \nabla p\right\} = 6\mu\left(\vec{V}.\nabla(ph)\right) + 12\mu\frac{\partial}{\partial t}(ph), \tag{11}$$

where ∇ is the gradient operator, p is the air pressure, h is the interfacial clearance, $\vec{V} = (V_x^t + V_x^r)\hat{i} + (V_y^t + V_y^r)\hat{j}$ is the total velocity vector representing the tape (^{t}) and roller velocities (^{r}), with the components in the x- and y-directions, μ is the dynamic viscosity of air, t is time, and Q_r is the flow rate correction coefficient due to slip-flow. This coefficient depends on the Knudsen number $Kn = \lambda/h$, and, for different slip-flow models it is defined as follows:

$Q_r = 1$,	classical compressible RE[10],
$Q_r = 1 + 6Kn$,	for 1st order slip-flow correction[6],
$Q_r = 1 + 6Kn + 6\,Kn^2$,	for 2nd order slip-flow correction[11],
$Q_r = f(Kn)$,	for Boltzman Reynolds equation[12].

The functional dependence of the flow correction for the Boltzman RE is derived by Fukui and Kaneko[13] and also presented by Crone et al. [7] For tape handling applications, the first order slip flow has been typically utilized.[24-28,28]

In case the web is permeable, the entrained air can diffuse through it. The lubrication flow can be modified to take this diffusion into account by using Darcy's law[14-16,37]. The resulting equation can be represented is follows:

$$\nabla.\left\{ph^3\nabla p\right\} - \frac{12\kappa_d}{c}p\left(p - p_a\right) = 6\mu\left(\vec{V}.\nabla(ph)\right) \tag{12}$$

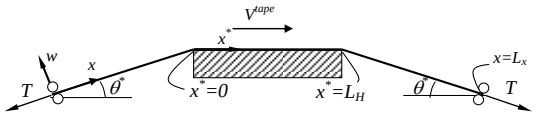

Figure 3. The flat-recording head configuration.

where κ_d is the permeability of the web, and p_a is the pressure of air at standard ambient conditions.

4. Examples of Modeling Results

In this section, four steady state fluid-structure interaction problems, which are encountered in different industrial uses of web handling, are presented. The goal here is to give an overview of the mechanics rather than draw conclusions based on effects of different parameters. References, where parametric studies were conducted, are cited as necessary.

4.1 Air-bar Applications

In both air- bar applications pressurized air is introduced between the flexible web and the rigid cylinder from the holes on the surface of the cylinder.[34,35,38] The air pressure and the web deflections are coupled. The air pressure is primarily balanced with respect to the belt-wrap pressure T/R, acting on the web due to the external tension. However, creating a flow pattern under the web which will balance the belt-wrap pressure is a challenging task. The air pressure and flow pattern primarily depends on the distribution pattern of the holes on the surface of the reverser. While the flow could stagnate in the central wrap region and provide an air cushion with a fairly uniform pressure, along the four edges of the wrap region air could flow from underneath the web with speeds reaching 25 - 30 m/s. Fig. 4 shows simulation results for a typical air-bar application. The web/air-bar clearance is found on the order of 3 mm and air pressure and flow variation under the web is presented.

4.2 Roller Results

4.2.1 Impermeable Webs

When a web is supported by a roller, the air entrainment causes mixed lubrication conditions in the web/roller interface.[8,9,14,15,16,40,45,46] The static equilibrium of the web requires that the belt-wrap pressure, T/R, to be balanced partially asperity contact pressure and partially by air pressure. With increasing web speed, the amount of entrained air and the magnitude of air pressure increases. Thus at higher transport velocities the share of the contact pressure on the equilibrium is reduced. Thus one can see, by considering Coulomb's friction law that the frictional force, $F_f = \mu_f F_n$, required to sustain high traction can be effectively reduced, without altering the value of the solid-to-solid coefficient of static friction, μ.. In fact, the effective friction coefficient μ_{fe} can be calculated from:

$$\mu_e = \ln(\Delta N / T + 1)/\theta_w \qquad (13)$$

where θ_w is the wrap angle and ΔN is the slip induced tension change.

Fig. 5 shows the contact pressure, air pressure, web/roller clearance and tension change for a 5 μm thick web traveling over a 6 mm diameter roller at 2 m/s transport speed. In this case the web is still in contact and the effective friction coefficient can be calculated from the tension change using the above formula.[40]

4.2.2 Permeable Webs

For a permeable web-material, air diffusion through the web reduces the amount of entrained air.[8,9,14,15,16,37] This phenomenon actually works in favor of keeping the effective friction coefficient high. Fig. 6 shows the web-roller clearance, air and contact

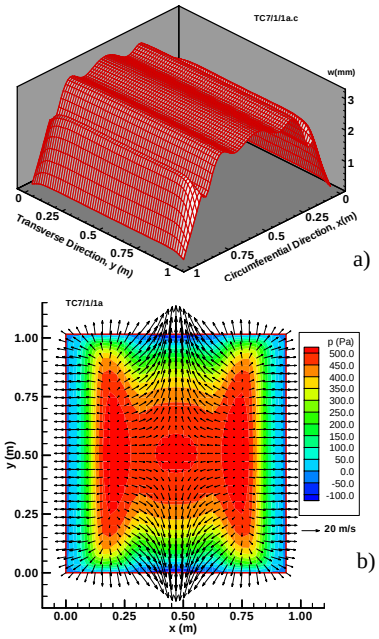

Figure 4. Simulation results for a) the web deflection $w(x,y)$ with respect to the undeflected web, and b) airflow pattern combined with air-pressure contours for an air-bar application.

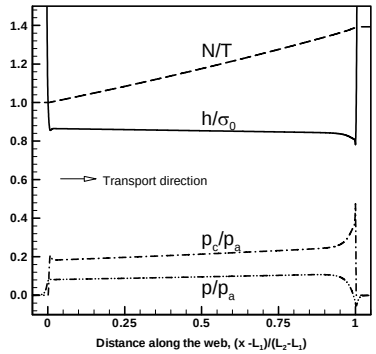

Figure 5. The tension N/T, web-roller clearance h/σ_0, contact pressure p_c/p_a, and air pressure p/p_a variation along a typical web roller interface, showing the mixed lubrication condition.

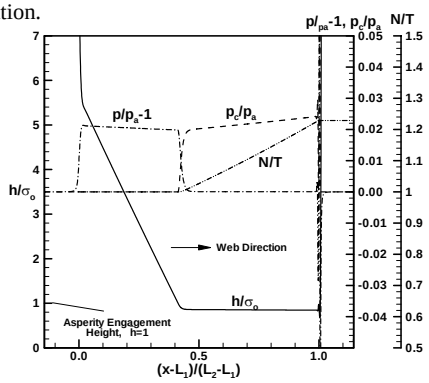

Figure 6. Typical simulation results for the interfacial conditions of a roller and a permeable web. Air pressure, p/p_a-1, contact pressure p_c/p_a, roller-web clearance h/σ_0 and tension N/T variation are plotted.

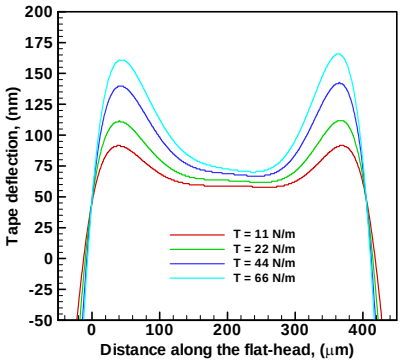

Figure 7. Simulation results of the head-to tape clearance over a 400 μm wide flat head for V = 2.54 m/s, and wrap angle of 2 deg.

pressures and tension change for a permeable web traveling over a roller. Three distinct regions can be identified. In the *entry region* air pressure is superambient and the web does not contact the roller, but the clearance h/σ_0 is diminishing almost linearly. In the *contact region*, the web and roller asperities are in contact; the contact pressure fully supports the web, and the air pressure is ambient. In the *exit region* typical sinusoidal air pressure distribution of the foil bearing peoblem is seen, where the air pressure undulates between superambient and subambient levels before finally reaching the ambient level. The contact pressure responds to this in order to keep the static equilibrium.

4.3 Flat Tape Recording Heads

There are several technical and commercial advantages to using flat-heads.[4,5,18,19,29,30,33,36] In particular, faster tape speeds over flat-heads have been shown to provide more reliable contact, in direct contrast to tape behavior over cylindrical heads. Moreover, the flat contour is more forgiving for tapes with different thickness, enabling backward/forward compatibility of tapes. Finally, flat-heads are considerably easier to manufacture as compared to contoured heads. Tape and head-wear at the corners of the head, and wear of the magnetic head regions are critical issues to be considered in designing a flat-head/tape interface.

A mathematical model of the head-tape interface showes that the contact is provided due to the *self-acting, subambient foil bearing* effect.[33] The analysis showed that air entrained in the flat-head/tape interface forms a subambient pressure layer, as the tape, wrapped over a flat surface, creates a diverging channel at the leading edge. The subambient air pressure over the flat-head region eventually pulls the tape down to contact the head.

Fig. 7 shows the tape/head clearance for indicated the operation parameters. The asperity height value of 48 nm is used in these calculations. This figure shows that the tape is bent down toward the head and settles near the surface. Mechanics of the tape in such an application is explained in reference.[39]

5. Summary

A review of the recent developments in the area of flexible media handling is presented, with particular emphasis to media-air interactions at steady state. This topic is expected to remain important as media transport speeds are pushed higher for production reasons. The general area of web handling research, is expected to take new turns with the requirements introduced by the RR manufacturing techniques for flexible displays. Media planarity, thermal stability, wrinkling, fatigue life of flexible displays, repeatability of depostion locations, effect of surface roughness on TFT deposition, are among the topics that are expected to be addressed.

References

1. Altman, H.C., Formulas for computing the stresses in center-wound rolls. TAPPI Journal Vol. 51 (1968), p.176-179.
2. Benson, R.C., The influence of web warpage on the lateral dynamics of webs. In Proceedings of the Fifth International Web Handling Conference, Oklahoma State University, June 1999.
3. Benson R.C., A nonlinear wound roll model allowing for large deformation. ASME J. of App. Mec. Vol. 62 (1994), p.853-859.
4. Biskeborn, R.G. and Eaton, J.H.. Flat-profile tape recording head. IEEE Transactions on Magnetics, Vol. 38, No. 5 (2002), p. 1919-1921.
5. Biskeborn, R.G. and Eaton, J.H., Hard-disk-drive technology heads for linear tape recording. IBM Journal of Research and Development, Vol. 47, No. 4 (2003), p.385-400.
6. Burgdofer, A., The Influence of Molecular Mean Free Path on the Performance of Hydrodynamic Gas Lubricated Bearings, Transactions ASME, Journal of Basic Engineering, Vol. 81, No. 1 (1959), p.94-100.
7. Crone, R.M, Jhon, M.S., Karis, T.E., and Bhushan. B., The behavior of a magnetic slider over a rigid disk surface: A comparison of several approximations of the modified Reynolds equations, Adv. Info. Storage Syst., Vol. 4 (1992), p.105-121.
8. Ducotey, K.S., Good, J.K., Predicting traction in web handling. ASME Journal of Tribology, Vol. 121 (1999), 618-624.
9. Ducotey, K. S. and Good, J. K., A numerical algorithm for determining the traction between a web and a circumferentially grooved roller, ASME Journal of Tribology, Trans ASME, Vol. 122 (2000), p.578-584.
10. Gross, W. A., (1980). Fluid Film Lubrication. John Wiley and Sons, New York.
11. Hsia, Y. T., and Domoto, G. A., An Experimental Investigation of Molecular Rarefaction Effects in Gas Lubricated Bearings at Ultra-Low Clearances, Transactions ASME, Vol. 105, (1983), p.120-130.
12. Fukui, S. and Kaneko, R., Analysis of Ultra-Thin Gas Film Lubrication Based on Linearized Boltzmann Equation: First report-Derivation of a Generalized Lubrication Equation Including Thermal Creep Flow, Trans. ASME Journal of Tribology, Vol. 110 (1988), p.253-261.
13. Fukui, S. and Kaneko, R., A database for interpolation of Poiseuille flow rates for high Knudsen number lubrication problems," Trans. ASME Journal of Tribology, Vol. 112 (1990), p. 78-83.
14. Hashimoto, H., Effects of foil bending rigidity on spacing height characteristics of hydrostatic porous foil bearings for web handling processes, Journal of Tribology, Trans ASME, Vol. 119 (1997), p.422-427.
15. Hashimoto, H., Air film thickness estimation, Journal of Tribology, Trans ASME, Vol. 121 (1999), p.50-55.
16. Hashimoto, H., Nakagawa, H., Improvement of web spacing and friction characteristics by two types of stationary guides. ASME Journal of Tribology Vol. 123 (2001), p.509-518.
17. Hakiel, Z., Nonlinear model for wound roll stresses. TAPPI Journal, May (1987), p.113-116.
18. Hinteregger H.F. and Müftü S., Contact tape recording with a flat-head contour. IEEE Transactions on Magnetics, Vol. 32, No. 5 (1996), p.3476-3478.
19. Hinteregger H.F. and Müftü S., Flat-heads for contact tape recording: performance measurements at different wrap-angles, tape speed and tape stiffness. Journal of Information Storage and Processing Systems, Vol. 2 (1999), p.75-82
20. Johnson, K.L., 1985, Contact Mechanics, Cambridge University Press

21. Jose, J. Taylor, R.J., de Callafon, R.A., Talke, F., Characterization of lateral tape motion and disturbances in the servo position error signal. Trib. Transactions, (2005) in press.
22. Keshavan, M., Wickert, J.A., Transient Discharge of Entrained Air From a Wound Roll, ASME Journal of Applied Mechanics, Vol. 65 (1998), p.804-810.
23. Koivurova, H. Pramila, A., Nonlinear vibration of axially moving membrane by finite element method. Computational Mechanics. Vol. 20 (1997), p.573-581.
24. Lacey, C.A., Talke, F.E. Measurement and Simulation of Partial Contact at the head/Tape Interface, Trans ASME Journal of Tribology, Vol. 114, No. 4 (1992), p.646-652.
25. Lacey, C.A., Talke, F.E., Simulation of Wear of Tape Head Contours, IEEE Trans. Mag., Vol. 28, No. 5 (1992), p.2554-2556.
26. Lakshmikumaran, A., Wickert, J., Equilibrium Analysis of Finite Width Foil-Bearings, ASME Journal of Tribology, Vol. 121 (1999), p.108-114.
27. Machida, T, Wickert, J., Lateral tape motion dynamics and simulation. Extended Abstracts, 13th Annual Symposium on ISPS, Santa Clara CA. Sponsored by ASME ISPS Division. (2001)
28. Müftü, S., Benson, R.C., A Study on Width-Wise Variations in the Two Dimensional Foil Bearing Problem, Transactions of the ASME, Journal of Tribology, Vol. 118, No.2 (1996), p.407-414.
29. Müftü, S., Hinteregger, H.F. Flat Heads for High Speed Contact Tape Recording: Experiments and Modelling of Wear and Performance, Proceedings of the I.S.P.S., ASME International Congress and Exposition, Atlanta, GA. November, (1996), p. 39-52.
30. Müftü, S. and Hinteregger H.F. The self-acting, subambient foil bearing in high speed, contact tape recording with a flat head, STLE Tribology Transactions, Vol. 41, No. 1 (1998), p.19-26.
31. Müftü, S., Lewis, T.S., Cole, K.A.. A numerical solution of the Euler's equations with nonlinear source terms in modeling the fluid dynamics of an air reverser. In Proceedings of the I.S.P.S., ASME International Congress and Exposition, Dallas, TX, November (1997), p. 39-48.
32. Müftü, S., Lewis, T.S., Cole, K.A., Benson, R.C., A two dimensional model of the fluid dynamics of an air reverser. ASME Journal of Applied Mechanics, Vol. 65 (1998), p.171-177.
33. Müftü, S. and Hinteregger H.F., The self-acting, subambient foil bearing in high speed, contact tape recording with a flat-head. STLE Tribology Transactions, Vol. 41, No. 1 (1998), p.19-26.
34. Müftü, S., Numerical solution of the equations governing the steady state of a thin cylindrical web supported by an air cushion. *Proceedings of the ASME Noise Control and Acoustics Division-1999* **NCA-26**, (1999), p.425-434.
35. Müftü, S., Cole, K.A., The fluid/structure interaction of a thin flexible cylindrical web supported by an air cushion. Journal of Fluids and Structures, Vol. 13 (1999), p.681-708.
36. Müftü S. and Donna Jean Kaiser, D. J., Measurements and Theoretical Predictions of Head/Tape Spacing over a Flat Head, *Tribology International*, Vol. 33 (2000), p.415-430.
37. Müftü, S., Altan, M.C., Mechanics of a porous web moving over a rigid guide. ASME Journal of Tribology. Vol. 122 (2000), 418-426.
38. Müftü, S., 2002. The mechanics of helically wrapped thin shell supported by an externally pressurized air cushion, Proceedings of FSI, AE & FIV+N Symposium ASME Winter Annual Meeting(2002).
39. Müftü, S. Tape mechanics over a flat recording head under uniform pull-down pressure, *Microsystem Technologies*, Vol. 9, No.8 (2003), p.546-554.
40. Müftü S. and Jagodnik, J.J., Traction between a web and a smooth roller, Trans ASME, Journal of Tribology, Vol. 126, No. 1 (2004), p.177-184.
41. Niemi, J. and Pramila, A., FEM-analysis of transverse vibrations of an axially moving membrane immersed in ideal fluid. International Journal for Numerical Methods in Engineering, Vol. 24 (1987), p.2301-2313.
42. Pramilla, A., Sheet flutter and interaction between sheet and air. Tappi Journal, Vol. 69 (1986), pp. 70-74.
43. Pramilla, A., Natural Frequencies of a submerged axially moving band. J Sound and Vib., Vol. 113 (1987), p.198-203.
44. Raman, A., Wolf, K.-D., Hagedorn, P., Observations on the vibrations of paper webs. In Proceedings of the Seventh International Web Handling Conference, Oklahoma State University, June (2001).
45. Rice, B.S. Cole K.A. and Müftü, S. , A Model for Determining the Asperity Engagement Height in Relation to Web Traction over Non-vented Rollers. Journal of Tribology, Trans. ASME, Vol. 124 (2002), p.584 - 594.
46. Rice, B.S. Reduction of Web-to-Roller Traction as a Result of Air Lubrication, PhD. Thesis, University of Rochester, Rochester, NY (2003).
47. Rongen, P. M. J., Finite Element Analysis of the Tape Scanner Interface in Helical Scan Recording. Ph.D. Dissertation, Technische Univesiteit Eindhoven, The Netherlands. (1994).
48. Shelton, J.J., Reid, K.N., Lateral dynamics of a real moving web. ASME Journal of Dynamic Systems, Measurement and Control Vol. 93 (1971), p.180-186.
49. Schilcting, H. (1987) Boundary-Layer Theory. New York: McGraw-Hill.
50. Tan, S. and Talke, F.E., Numerical and experimental investigations of the head/tape interface in a digital linear tape drive. Journal of Tribology, Trans. ASME, Vol. 123 (2001), p.343-349.
51. Taylor, R.J., Talke, F., Investigation of roller interactions with flexible tape medium. Trib. Trans., in press. (2005).
52. Timoshenko, S.P., Woinkowsky-Krieger, S., (1987) Theory of Plates and Shells. McGraw-Hill, New York.
53. Wickert, J.A., Mote, C.D., Current research on the vibration and stability of axially-moving materials. Shock and Vibration Digest Vol. 20 (1988), p.3-13.
54. Lee, Y.M., Wickert, J.A., Stress Field in Finite Width Axisymmetric Wound Rolls. ASME Journal of Applied Mechanics, Vol. 69, No. 2 (2002), p.130-138.
55. Wu, Y., Talke, F., The Effect of Surface Roughness on the Head-tape Interface, Journal of Tribology, Trans ASME, Vol. 118, No. 2 (1996), p.376-381.
56. Zhu, J. and Talke, F.E., Optimal design of the magnetic tape head, J. Info. Storage Proc. Syst., Vol. 3 (2001), p.121-130.
57. Zhu, J., Baugh, E. and Talke, F.E., Measurement of magnetic tape asperity compliance using five-length interferometry. J. Info. Storage Proc. Syst., Vol. 3 (2001), p.161-168.